TECHNISCHE UNIVERSITÄT
BERGAKADEMIE FREIBERG
Die Ressourcenuniversität. Seit 1765.

First principles based interatomic potential generation for magnetic Iron



Master Thesis | Praveenkumar Hiremath - 57955.

Supervisors:

Prof. Dr. Jens Kortus | M.Sc Sebastian Schwalbe

Outline

- Introduction
  - Why interatomic potential for iron?
  - First principles method-DFT.
  - Potfit package.
  - Angular Dependent Potential.
- Prescription
  - DFT data set.
  - Elk output conversion.
  - Potfit potential generation.
  - Testing the quality of potfit potential.
- Results
- Conclusion and future work

Why interatomic potential for iron?

- Iron originates in stars and is a supernova remnant.
- Iron causes earth's magnetic filed.
- Iron alloys- elinvar, invar, various types of steels etc.
- Wide range applications of iron and its alloys.
    - Elinvar- balance springs for mechanical watches and chronometers.
    - Invar- motor valves, precision instruments, clocks, anti-magnetic watches, seismic creep gauges etc.
    - Iron and steel - construction industries, roads and railways, aerospace industry, ship building, heavy equipments like bulldozers, automobile industry, cooking utensils, surgical instruments and so on.
- Accuracy of molecular dynamics simulations.
- Inadequacy of reliable interatomic potentials.
    - Crack propagation analysis in α-iron[1].
- Importance of magnetism.
    - Tight binding study performed by Guoqiang Liu et.al.[2].

First principles method-DFT

- Hamiltonian operator for many-body time-independent Schrödinger equation [3].

$$\hat{H} = -\frac{\hbar^2}{2m_e}\sum_i \nabla_i^2 - \frac{\hbar^2}{2M_I}\sum_I \nabla_I^2 - \sum_{i,I}\frac{Z_I e^2}{|r_i - R_I|} + \frac{1}{2}\sum_{i\neq j}\frac{e^2}{|r_i - r_j|} + \frac{1}{2}\sum_{I\neq J}\frac{Z_I Z_J e^2}{|R_I - R_J|} = T_e + T_N + V_{Ne}(r,R) + V_{ee}(r) + V_{NN}(R)$$

- Using Born-Oppenheimer approximation, T_N can be set to zero.
- Hence ,the many-body time-independent Schrödinger equation.

$$\hat{H}\,|\Psi_i(r)\rangle = E\,|\Psi_i(r)\rangle$$

- Solving above Schrödinger equation is not feasible.

First principles method-DFT

- Hence to solve a non-relativistic many-body system, density functional theory (DFT) is used.
- The works of Pierre Hohenberg , Walter Kohn and Lu Jeu Sham lead to DFT.
- DFT uses electron densities which are defined using Kohn - Sham wavefunctions.
- To calculate the ground state energy of a system, an approximate E_{XC} functional determining exchange-correlation energy of electrons, is used (GGA, LDA, Hybrid functionals).

Potfit package

- Potfit uses force-matching algorithm to generate inter atomic potentials with first principles data as reference [4].
- Designed primarily to use VASP output as reference data.
- Potfit requires three input files.
  - Initial potential file.
  - Parameter file.
  - Configuration file.
- Number of analytic functions to be used in initial potential file for an ADP potential generation is N(3N+7)/2.
- Here for a chosen interaction model, potential generation involves two major tasks.
  - Use force-matching algorithm to calculate potential at every parameter set.
  - Parameterize the potential model by optimizing/minimizing the target function thus providing optimized parameter set.

Potfit package

- Target function is optimized using different optimization algorithms.
- Optimization algorithms used are
  - Simulated annealing.
  - Differential evolution.
  - Powell's least square method(conjugate gradient).
- Target function[4].

$$Z(\boldsymbol{\xi}) = Z_F(\boldsymbol{\xi}) + Z_C(\boldsymbol{\xi}),$$

where

$$Z_F(\boldsymbol{\xi}) = \sum_{k=1}^{m} u_k (F_k(\boldsymbol{\xi}) - F_k^0)^2,$$

$$Z_C(\boldsymbol{\xi}) = \sum_{r=1}^{N_c} w_r (A_r(\boldsymbol{\xi}) - A_r^0)^2.$$

Potfit package

- Potfit Flowchart [4].

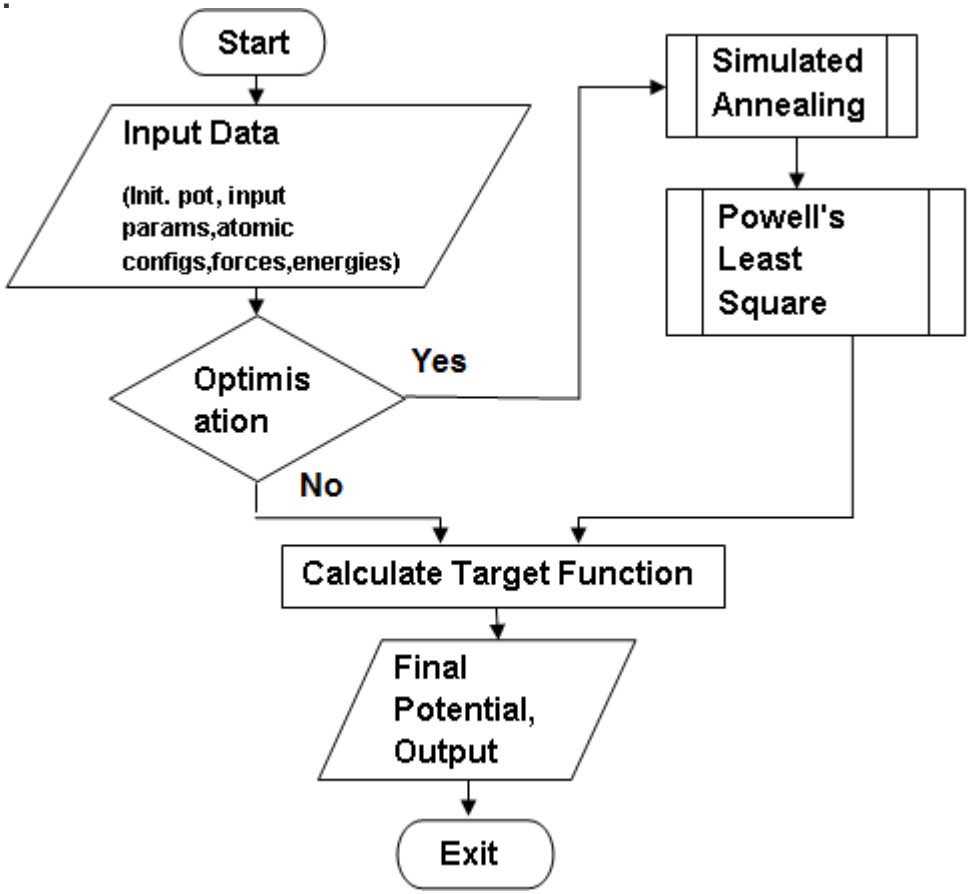

Angular Dependent Potential

- Formalism.

$$E_{\mathrm{tot}} = \frac{1}{2}\sum_{i,j;i\neq j}^{N}\Phi_{\mathrm{ij}}(r_{\mathrm{ij}}) + \sum_{i}F_{\mathrm{i}}(n_{\mathrm{i}}) + \frac{1}{2}\sum_{i,\alpha}(\mu_{\mathrm{i}}{}^{\alpha})^2 + \frac{1}{2}\sum_{i,\alpha,\beta}(\lambda_{\mathrm{i}}{}^{\alpha\beta})^2 - \frac{1}{6}\sum_{i}\nu_{\mathrm{i}}{}^2$$

- The first $\Phi_{ij}(r_{ij})$ represents pair interaction.
- The second term $F_i(n_i)$ represents embedding function.
- The third μ_i^{α}, fourth $\lambda_i^{\alpha\beta}$ and fifth v_i terms represent vectors, tensors and trace of $\lambda_i^{\alpha\beta}$.respectively.

DFT data set

- Elk FP-LAPW code is used [5].
- Allotropes of iron under consideration: α-iron – FM, AFM, NM, γ-iron – AFM, NM, ε-iron –FM, AFM, NM.
- E_{XC} functional GGA-PBE [6] is used.
- *E(V)* curves are obtained just around the equilibrium volume (quadratic region) using spinpolarized calculations.
- The configurations resulting in *E(V)* curves form the reference data set for potfit.
- Verify the nature of *E(V)* and *E(M)* curves.
- Calculate cohesive energies of all configurations.
- Cohesive energy is calculated as

E_{coh} = *Isolated Fe atom energy – Fe atom energy in crystal.*

Elk output conversion

- Potfit is compatible with VASP output format.
- Hence, elk output should be converted to potfit compatible format.
- Units of force, cohesive energy, geometry information in potfit input files are eV/Å, eV, Å respectively.

Potfit potential generation

- To generate ADP potential, represent the five interaction terms of ADP formalism using analytic functions ‘eopp’ (empirical oscillating potentials) [7] , ‘csw2’ [8] , ‘bjs’ [9].

’eopp’ with six parameters

$$V(r) = \frac{C_1}{r^{\eta}{}_1} + \frac{C_2}{r^{\eta}{}_2} cos(kr + \varphi)$$

’csw2’ with four parameters

$$\rho(r) = \frac{1 + a_1 cos(\alpha r + \varphi)}{r^{\beta}}$$

’bjs’ with three parameters

$$F(n) = F_0[1 - \gamma \ln n]n^{\gamma} + F_1 n$$

Potfit potential generation

- Initialize the parameter set i.e initial potential file.
- Configuration and parameter files are prepared.
- Configuration file contains reference data from DFT and parameter file contains input parameters like optimization methods, energy and stress weights, output potential format, number of steps and so on.
- Here, simulated annealing and Powell's least square method are used.
- Force weight of '1' and energy weight of '100' are used in this work.
- Vary the parameter for annealing temperature, parameter set and reference data set (if needed) until satisfactory potential is obtained.
- Test the potential through molecular dynamics calculations.

Testing the quality of potfit potential

- LAMMPS [10] package is used to perform MD calculations.
- MD calculations performed.
  - Cohesive energy and lattice parameter.
  - *E(V)* curves.
  - Elastic constants.
  - Relaxed monovacancy formation energy.
  - Surface energies ($E_{(100)}$, $E_{(110)}$,$E_{(111)}$ in α and γ iron).
  - Generalized stacking fault energy curve (GSFE curve for α-iron).

Results-DFT data set

- Equilibrium properties of relaxed structures.

Strcuture	V_0	$E_{0,coh}$	B_0	Ref. V_0	Ref. $E_{0,coh}$	Ref. B_0
-	$Å^3$	eV/atom	Gpa	$Å^3$	eV/atom	Gpa
bcc-NM	10.478	-3.49	269.94	10.35[11]	-	288[11]
bcc-FM	11.465	-4.11	181.14	11.36[12]	-4.28[12]	189[12]
bcc-AFM	11.514	-3.96	190.98	10.97[13]	-	176[13]
fcc-NM	10.17	-3.90	278.94	10.33[11]	-	283[11]
fcc-AFM	11.26	-4.11	142.29	11.30[12]	-	133[12]
hcp-NM	10.12	-3.96	293.31	10.23[11]	-	292[11]
hcp-FM	10.12	-3.94	292.59	10.55[11]	-	241[11]
hcp-AFM	10.383	-3.97	233.72	10.43[14]	-	213[14]

Results-DFT data set

- The FM α-iron study.
- *E(V)* curve.

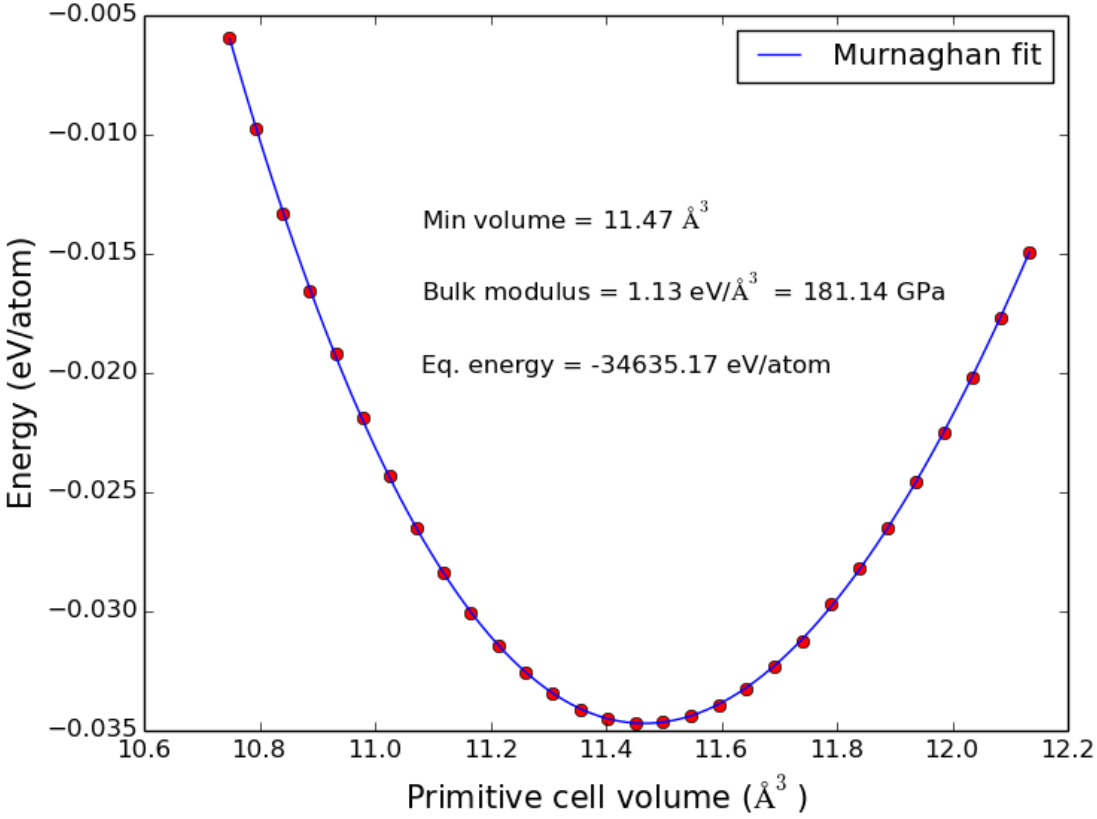

Results-DFT data set

- The FM α-iron study.
- *E(M)* curve.

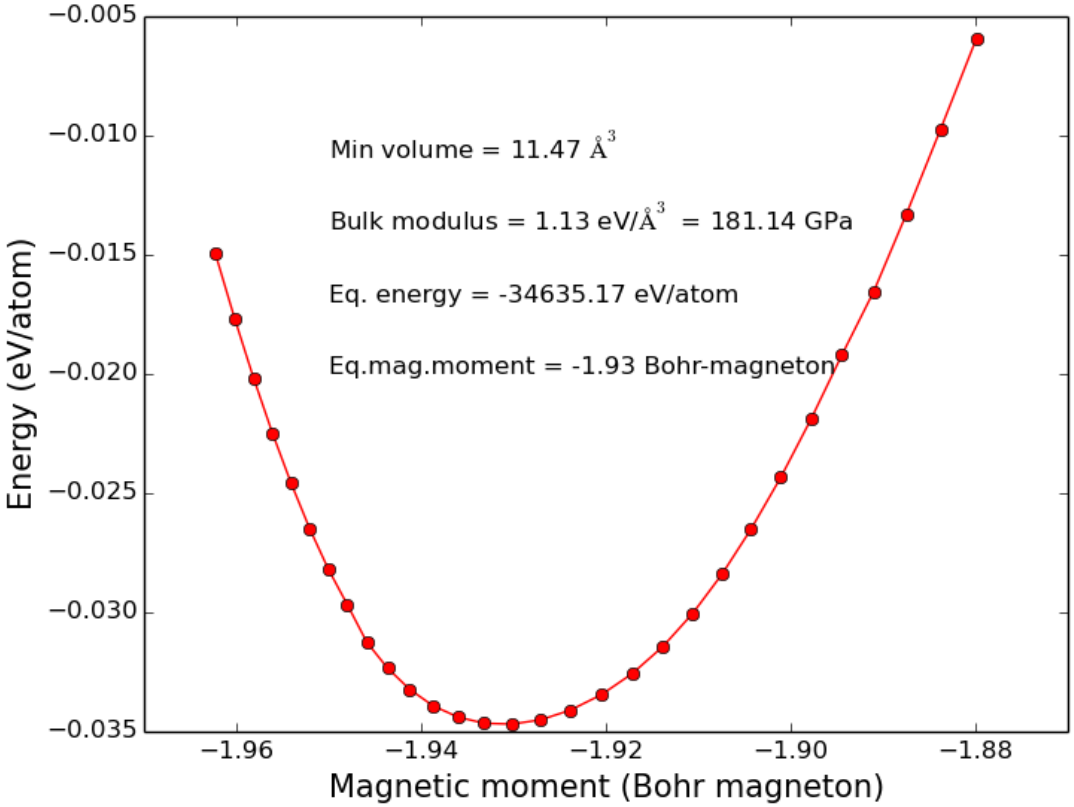

Results-DFT data set

- The FM α-iron to NM ε-iron phase transition study[15].

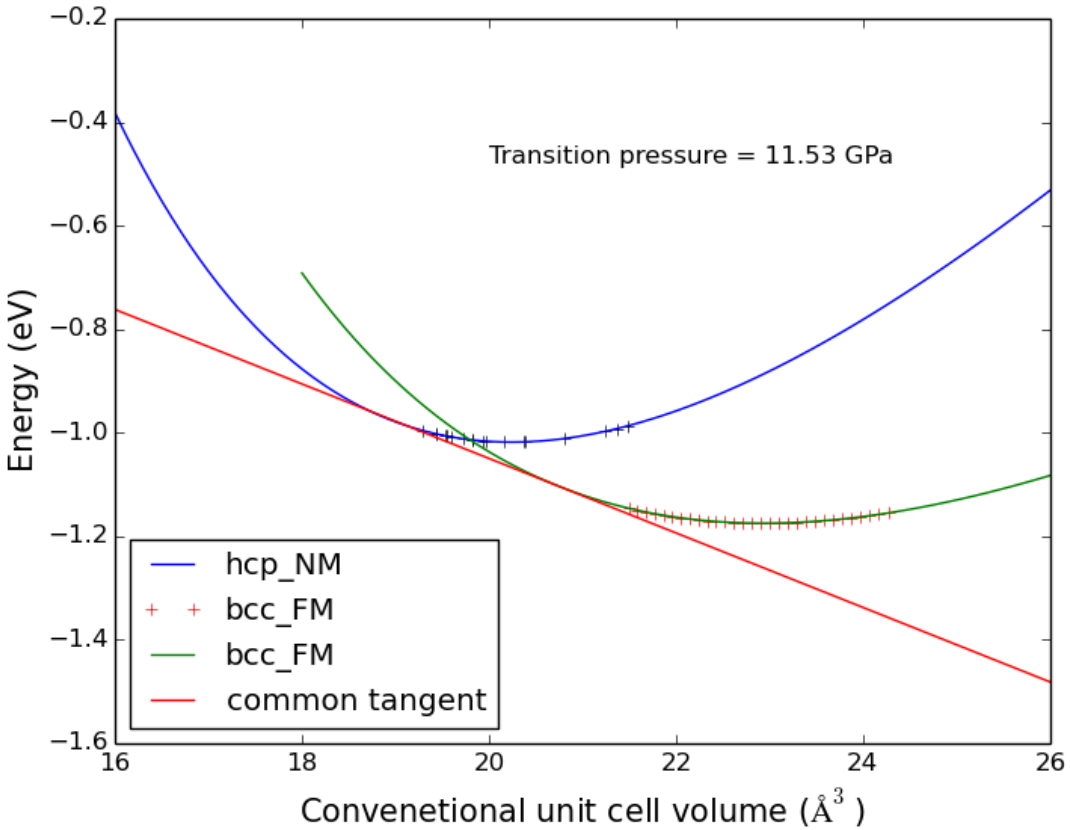

Results-Potfit potential for α-iron.

- Some potentials reproduce elastic constants very accurately but fail to reproduce surface energies.
- Some other potentials reproduce elastic constants poorly and reproduce the ordering of surface energies precisely but not the magnitudes of surface energies.
- So of all the α-iron potentials generated in this work, potential „T2-M4-43“ behaves pretty well in all the cases.
- Comparison of properties calculated with potential „T2-M4-43“ and reference results is shown in following table.

Results-Potfit potential for α-iron.

Properties	Units	T2-M4-43 pot	Reference
E_{coh}	eV/atom	-4.07	-4.28[16]
V_0	Å^3	11.42	11.78^{Expt}[16]
C_{11}	Gpa	248.71	242^{Expt}[16]
C_{12}	Gpa	161.15	146.5^{Expt}[16]
C_{44}	Gpa	119.53	112^{Expt}[16]
B_0	Gpa	190.34	189^{DFT} [12]
SM-I	Gpa	119.53	-
SM-II	Gpa	43.78	-
μ	Gpa	0.393	-
E_{vac}	eV/atom	1.22	1.53[16]
$E_{(100)}$	J/m^2	3.30	2.463^{MD}[16]
$E_{(110)}$	J/m^2	3.213	2.358^{MD}[16]
$E_{(111)}$	J/m^2	3.56	2.658^{MD}[16]

Results-Potfit potential for α-iron.

- Generalized stacking fault energy curve.

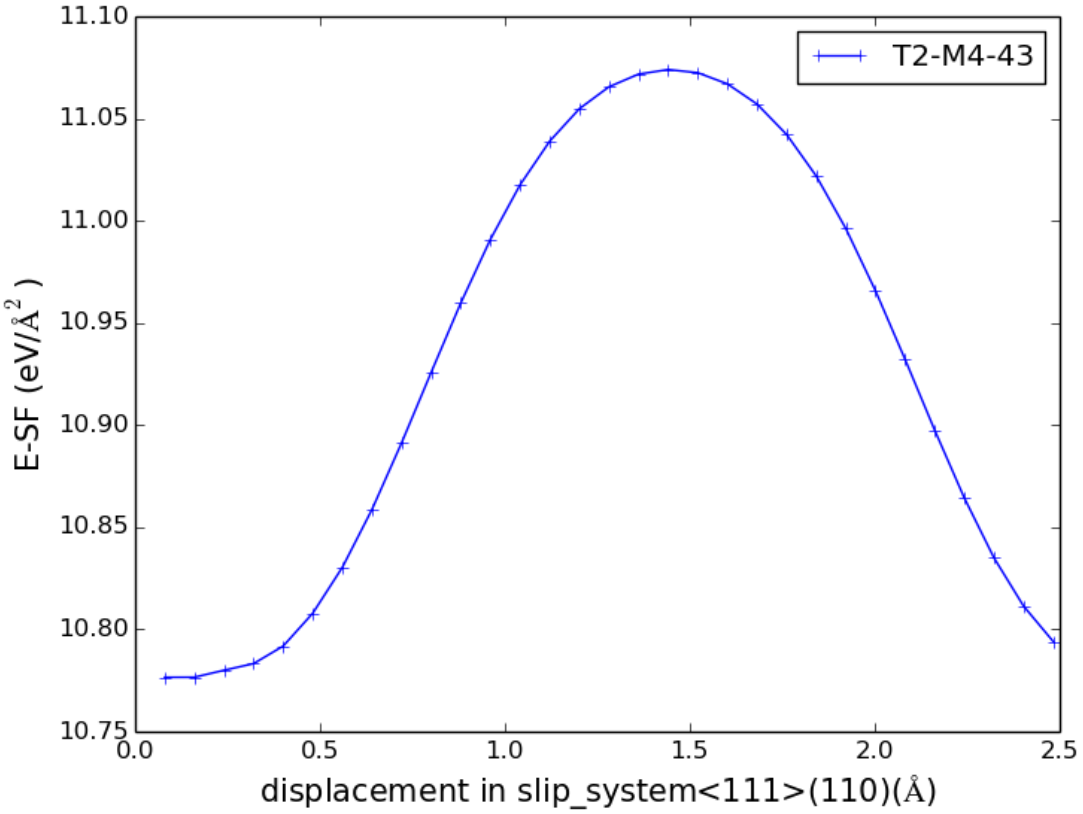

Results-Potfit potential for α-iron.

- Comparison of GSFE using potfit potential T2-M4-43 and Finnis Sinclair potential [18].

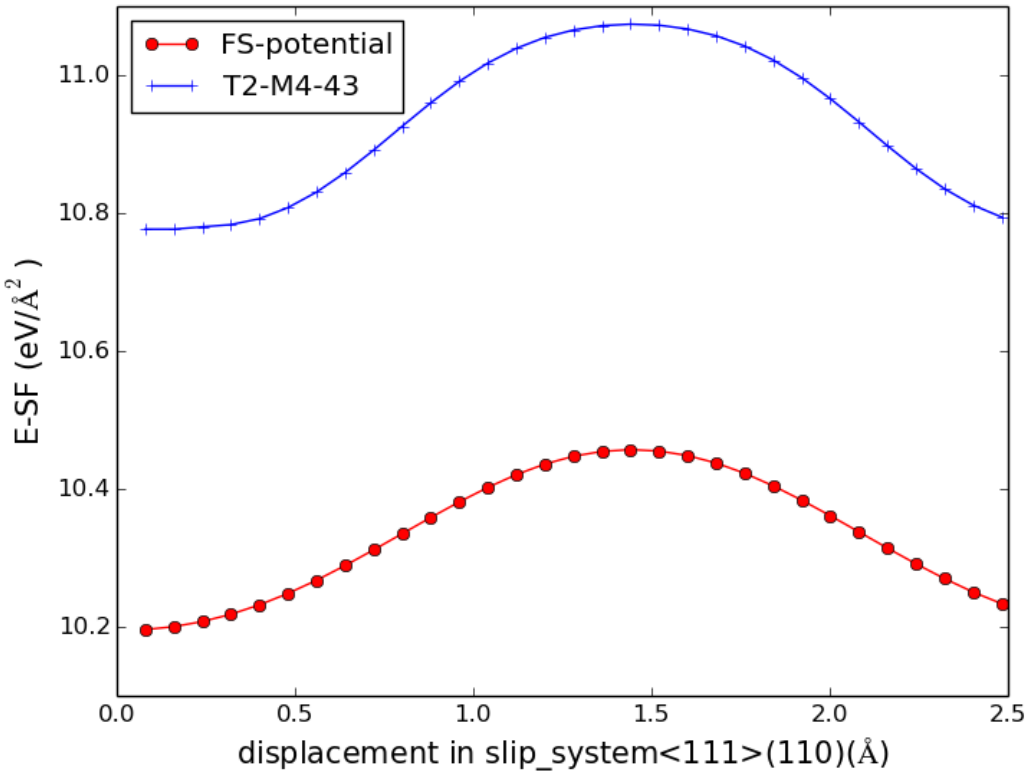

Results-Potfit potential for γ-iron.

- Just as in the case of α-iron potentials, of all the γ-iron potentials generated in this work, potential „T22-M6-2“ behaves pretty well in all the cases and is comparable to Analytic Bond Order Potential(ABOP) developed by M Müller et.al [12].

- Comparison of properties calculated with potential „T22-M6-2“ and ABOP, reference results is shown in following table.

Results-Potfit potential for γ-iron.

Properties	Units	T22-M6-2 pot	Reference
E_{coh}	eV/atom	-4.11	-
V_0	Å^3	11.25	11.3^{ABOP} [12]
C_{11}	Gpa	217.5	204^{ABOP} [12]
C_{12}	Gpa	149.096	144^{ABOP} [12]
C_{44}	Gpa	115.125	101^{ABOP}[12]
B_0	Gpa	171.89	164^{DFT} [12]
SM-I	Gpa	115.125	-
SM-II	Gpa	34.2	-
μ	Gpa	0.406	-
E_{vac}	eV/atom	1.128	1.7^{Expt} [16]
$E_{(100)}$	J/m^2	1.678	2.463^{MD}[16]
$E_{(110)}$	J/m^2	2.429	2.358^{MD}[16]
$E_{(111)}$	J/m^2	1.397	2.658^{MD}[16]

Results-Potfit potential for ε-iron.

- Potfit generated –iron potential „T30-M5-1“ is tested only for elastic constants, *E(V)* curve.

Properties	Units	T30-M5-1 pot	Reference
E_{coh}	eV/atom	-4.09	-
V_0	Å^3	21.5	20.46^{DFT} [17]
C_{11}	Gpa	501.94	556^{DFT} [17]
C_{12}	Gpa	364.83	300^{Expt} [17]
C_{44}	Gpa	61.54	248^{DFT}[17]
C_{33}	Gpa	662.51	647^{DFT} [17]
C_{13}	Gpa	162.77	143^{DFT}[17]
C_{66}	Gpa	68.47	
B_0	Gpa	263.16	297^{DFT}[17]

Results-MD surface energy calculation.

- Three different surface energy calculation methods have been employed.
  - Method of calculation using sufficient layers along direction of surface.
  - Periodic slab geometry method.
  - Intercept method.

- All these methods are congruent i.e yield similar results for surface energies.

Conclusion

- Some reference data which cannot be obtained from experimental procedures can be calculated using DFT with better accuracy.
- Hence, large amount of information can be used as reference data for potfit making it possible to generate more realistic interatomic potential for MD calculations.
- Application of apt zeeman field during spinpolarized calculation is paramount for obtaining correcting magnetic phase with correct equilibrium magnetic moment.
- FM γ-iron spinpolarized and FSM calculations indicate the existence of non-collinear magnetism.
- GGA-PBE functional is not non-collinear unlike LSDA and hence it poses convergence problems in non-collinear spinpolarized calculations.
- Importance of 3d-electrons which are shielded by only two 4s electrons.

Conclusion

- Quality of potfit generated potential depends on quality of reference data from DFT.
- Optimization algorithms like simulated annealing help to obtain a better global minimum thereby facilitating generation of more realistic interatomic potentials.
- Introduction of a self-consistent electron density term in potential model might be the key for generating a common potential for different phases of iron.
- Transferability of potential depends on the configurations in reference data set.

Future work

- If different defect energies are calculated in DFT and used as part of reference data in potfit, a very good potential can be obtained. Then it is possible to use this potential to understand crack propagation behaviour.
- It would also be easier to optimize the parameters corresponding to non-central bonding terms in ADP formalism if defect energies are included in reference data.

References:

[1] Johannes J Möller and Erik Bitzek. Comparative study of embedded atom potentials for atomistic simulations of fracture in α-iron. *Modelling and simulation in Material Science and Engineering,* 22(4):045002, 2014.

[2] Guoqiang Liu, D Nguyen-Manh, Bang-Gui Liu, and DG Pettifor. Magnetic properties of point defects in iron within the tight-binding-bond stoner model. *Physical Review B,* 71(17):174115, 2005.

[3] Richard M Martin. *Electronic structure: basic theory and practical methods.* Cambridge university press, 2004.

[4] Peter Brommer, Alexander Kiselev, Daniel Schopf, Philipp Beck, Johannes Roth, and Hans-Rainer Trebin. Classical interaction potentials for diverse materials from ab initio data: a review of potfit. *Modelling and Simulation in Materials Science and Engineering*, 23(7):074002, 2015.

References:

[5] Kay Dewhurst, S Sharma, L Nordstrom, F Cricchio, F Bultmark, H Gross, C Ambrosch-Draxl, C Persson, C Brouder, R Armiento, et al. The elk fp-lapw code. ELK, *http://elk.sourceforge.net*, 2016.

[6] John P Perdew, Kieron Burke, and Matthias Ernzerhof. Generalized gradient approximation made simple. *Physical review letters*, 77(18):3865, 1996.

[7] Marek Mihalkovic and CL Henley. Empirical oscillating potentials for alloys from ab initio fits and the prediction of quasicrystal-related structures in the al-cu-sc system. Physical Review B, 85(9):092102, 2012.

[8] Amitava Banerjea and John R Smith. Origins of the universal binding-energy relation. Physical Review B, 37(12):6632, 1988.

References:

[9] Somchart Chantasiriwan and Frederick Milstein. Higher-order elasticity of cubic metals in the embedded-atom method. Physical Review B, 53(21):14080, 1996.

[10] Steve Plimpton, Paul Crozier, and Aidan Thompson. Lammps-large-scale atomic/molecular massively parallel simulator. *Sandia National Laboratories*,18,2007.

[11] Zhao-Yi Zeng, Cui-E Hu, Xiang-Rong Chen, Ling-Cang Cai, and Fu-Qian Jing.Magnetism and phase transitions of iron under pressure. *Journal of Physics:Condensed Matter*, 20(42):425217, 2008.

[12] Michael Müller, Paul Erhart, and Karsten Albe. Analytic bond-order potential for bcc and fcc iron—comparison with established embedded-atom method potentials. Journal of Physics: Condensed Matter, 19(32):326220, 2007.

References:

[13] HC Herper, E Hoffmann, and P Entel. Ab initio full-potential study of the structural and magnetic phase stability of iron. Physical Review B, 60(6):3839, 1999.

[14] Gerd Steinle-Neumann, RE Cohen, and Lars Stixrude. Magnetism in iron as a function of pressure. Journal of Physics: Condensed Matter, 16(14):S1109,2004.

[15] RF Smith, JH Eggert, DC Swift, J Wang, TS Duffy, DG Braun, RE Rudd, DB Reisman, JP Davis, MD Knudson, et al. Time-dependence of the alpha to epsilon phase transformation in iron. J. Appl. Phys, 114(22):223507, 2013.

References:

[16] H Chamati, NI Papanicolaou, Y Mishin, and DA Papaconstantopoulos. Embedded-atom potential for fe and its application to self-diffusion on fe (100). *Surface Science*, 600(9):1793–1803, 2006.

[17] GY Guo and HH Wang. Gradient-corrected density functional calculation of elastic constants of fe, co and ni in bcc, fcc and hcp structures. *Chinese Journal of Physics*, 38(5):949–961, 2000.

[18] Graeme J. Ackland. Finnis-sinclair potential for bcc iron in eam format. https://openkim.org/cite/MO_142799717516_002, 2016. Online; accessed: 2016-10-29.

References:

[19] Zhao-Yi Zeng, Cui-E Hu, Xiang-Rong Chen, Ling-Cang Cai, and Fu-Qian Jing.Magnetism and phase transitions of iron under pressure. *Journal of Physics:Condensed Matter*, 20(42):425217, 2008.

Appendix

- FM γ-iron is studied using LSDA E_{XC} functional.
- HS-phase *E(V)* curve

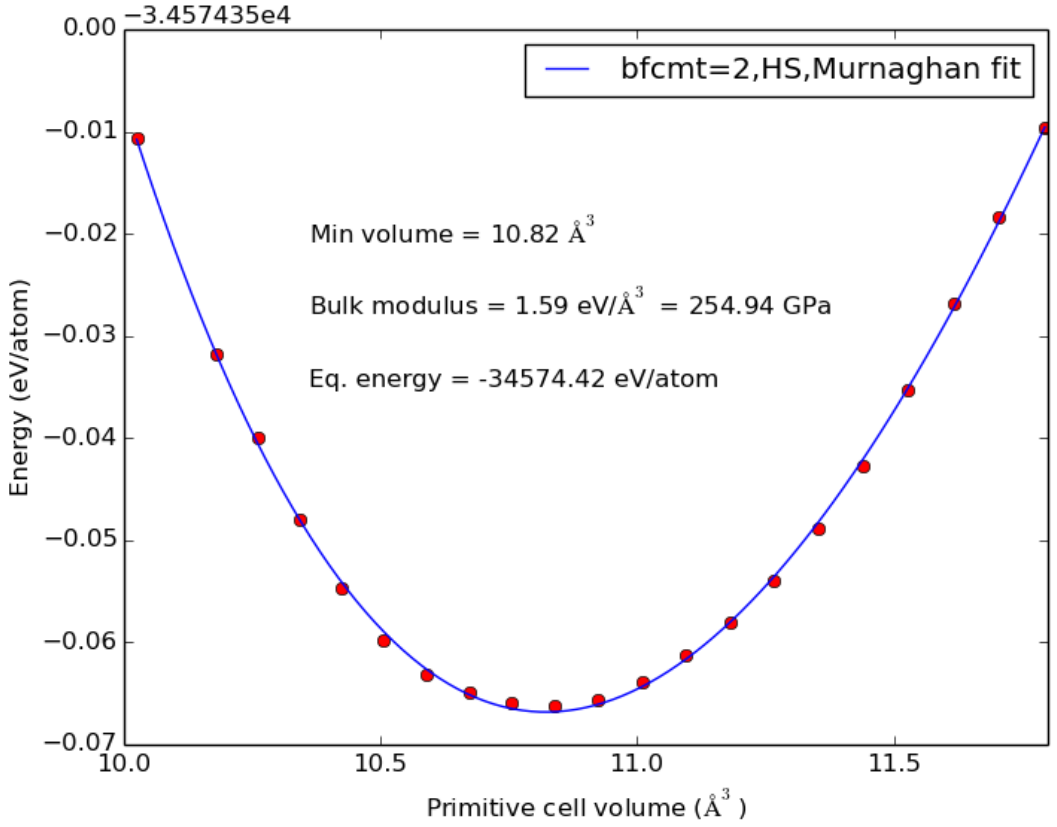

Appendix

- FM γ-iron is studied using LSDA E_{XC} functional.
- HS-phase *E(M)* curve

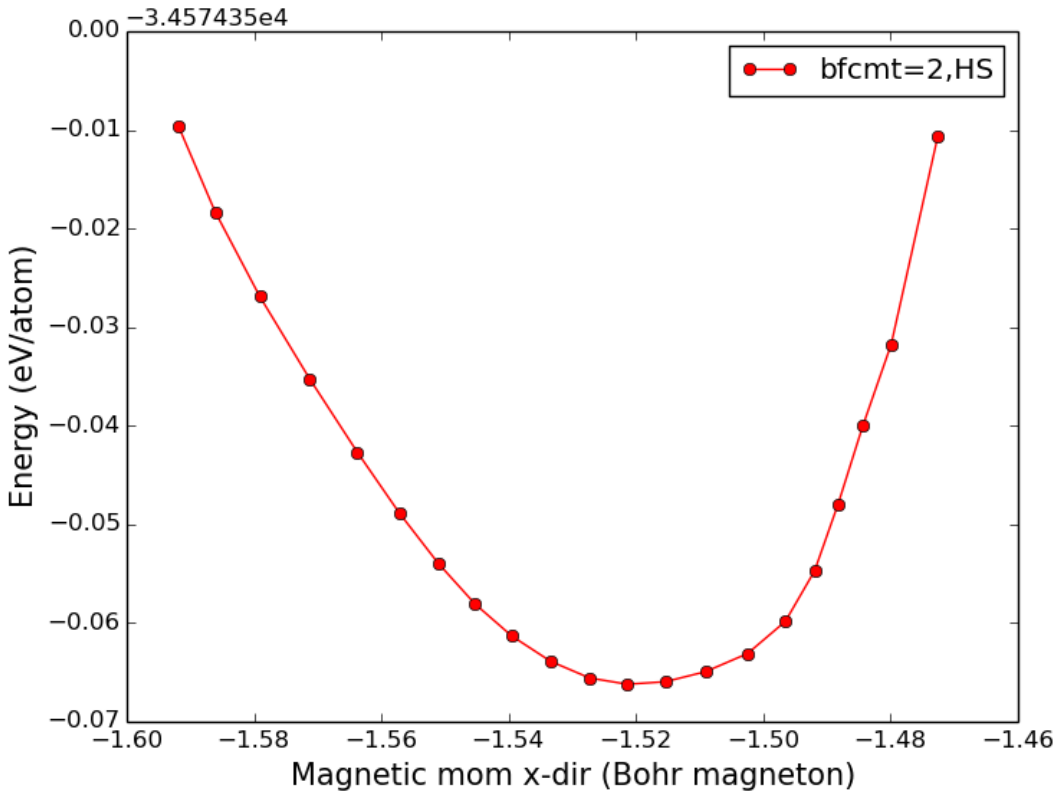

Appendix

- FM γ-iron is study.
- Here, equilibrium volume of 10.89 $Å^3$ (primitive cell), bulk modulus of 254.94 Gpa and magnetic moment of 2.64 μ_B are observed.
- These are in agreement with other first principles results [19].

Thank You